AGU PUBLICATIONS

JGR

Journal of Geophysical Research: Solid Earth

RESEARCH ARTICLE
10.1002/2017JB014456

Key Points:
- Pore pressure modeling of injection from 22 wastewater disposal wells within 30 km of seismicity
- Injection from Far-field Wells between 15 and 30 km contributes a significant portion of pore pressure increase near the induced seismicity
- Reduction of spatially aggregated injection rate by decrease of individual rates or farther well spacing may be more effective mitigation

Correspondence to:
M. R. M. Brown,
megan.r.brown@colorado.edu

Citation:
Brown, M. R. M., S. Ge, A. F. Sheehan, and J. S. Nakai (2017), Evaluating the effectiveness of induced seismicity mitigation: Numerical modeling of wastewater injection near Greeley, Colorado, *J. Geophys. Res. Solid Earth*, *122*, 6569–6582, doi:10.1002/2017JB014456.

Received 18 MAY 2017
Accepted 31 JUL 2017
Accepted article online 4 AUG 2017
Published online 24 AUG 2017

Evaluating the effectiveness of induced seismicity mitigation: Numerical modeling of wastewater injection near Greeley, Colorado

Megan R. M. Brown[1], Shemin Ge[1], Anne F. Sheehan[1,2], and Jenny S. Nakai[1,2]

[1]Department of Geological Sciences, University of Colorado Boulder, Boulder, Colorado, USA, [2]Cooperative Institute for Research in Environmental Sciences, University of Colorado Boulder, Boulder, Colorado, USA

Abstract Mitigation of injection-induced seismicity in Greeley, Colorado, is based largely on proximity of wastewater disposal wells to seismicity and consists of cementation of the bottom of wells to eliminate connection between the disposal interval and crystalline basement. Brief injection rate reductions followed felt events, but injection rates returned to high levels, >250,000 barrels/month, within 6 months. While brief rate reduction reduces seismicity in the short term, overall seismicity is not reduced. We examine contributions to pore pressure change by injection from 22 wells within 30 km of the center of seismicity. The combined injection rate of seven disposal wells within 15 km of the seismicity (Greeley Wells) is correlated with the seismicity rate. We find that injection from NGL-C4A, the well previously suspected as the likely cause of the induced seismicity, is responsible for ~28% of pore pressure increase. The other six Greeley Wells contribute ~28% of pore pressure increase, and the 15 Far-field Wells between 15 and 30 km from the seismicity contribute ~44% of pore pressure increase. Modeling results show that NGL-C4A plays the largest role in increased pore pressure but shows that the six other Greeley Wells have approximately the same influence as NGL-C4A. Furthermore, the 15 Far-field Wells have significant influence on pore pressure near the seismicity. Since the main mitigation action of cementing the bottom of wells has not decreased seismicity, mitigation based on reduced injection rates and spacing wells farther apart would likely have a higher potential for success.

1. Introduction

The occurrence of wastewater injection-induced seismicity has been recognized since the Denver earthquakes at the Rocky Mountain Arsenal starting in the 1960s [*Healy et al*., 1968; *Hsieh and Bredehoeft*, 1981]. When wastewater disposal well injection causes pore pressure increase along preexisting, critically stressed faults, the effective normal stress is reduced and an induced earthquake can occur. Even though this mechanism has been accepted for decades [*Healy et al*., 1968; *Raleigh et al*., 1976; *Ellsworth*, 2013], how to respond and mitigate induced seismicity is still debated. The focus of mitigation, to date, has mostly been on temporarily stopping or reducing the injection as a way to control the seismicity. *Raleigh et al*. [1976] showed the feasibility of changing injection parameters, injection/extraction rates, and locations, to control seismicity with the Rangely, Colorado, experiments. Mandates for the reduction of injection rates have been used in Oklahoma and may be effective in lowering the total number of seismic events of magnitude $M > 3.0$ [*Langenbruch and Zoback*, 2016]. However, several large-magnitude earthquakes, including the Pawnee, Oklahoma, moment magnitude M_w 5.8 earthquake, the largest in Oklahoma's instrumental record, occurred after the mandated injection reduction [*Yeck et al*., 2017]. Generally, attempts to control the seismicity via controlling injection have not been effective overall [*Bommer et al*., 2015], especially in enhanced geothermal projects where the largest magnitude earthquakes often occur following the shut-in (stopping of injection/pumping) of the wells. The largest earthquake, an M_w 3.9, in a series of wastewater injection-induced earthquakes in Youngstown, Ohio, occurred within 24 h of the cessation of the injection [*Kim*, 2013]. *Bommer et al*. [2015] suggest a fundamentally different approach to induced seismicity mitigation based on changes to all elements of risk like exposure (e.g., amount of buildings, infrastructure, and people in area of possible shaking) and vulnerability (e.g., susceptibility of structures to damage or adverse consequences). That is, mitigation is not necessarily focused on stopping or even reducing seismicity, but in reducing the risk to communities.

Mitigation actions fall into two categories: preventative measures and reactive measures. Wastewater disposal wells are permitted under the Environmental Protection Agency's Underground Injection Control

Program, but state agencies often have the regulatory authority. Preventative measures are taken during the permitting process for new wells. Preventative measures may include well spacing requirements to reduce the possibility of combined influence of injection from multiple wells; well siting away from critical infrastructure, population centers, and high-risk facilities; and identification of known earthquake sources (past earthquake locations and known faults). The Colorado regulatory agency, the Colorado Oil and Gas Conservation Commission (COGCC), requires a review of seismicity potential using the Colorado Geological Survey earthquake databases and published maps, United States Geological Survey (USGS) earthquake databases and maps, and other known fault maps [*Colorado Oil and Gas Conservation Commission* (*COGCC)*, 2016]. In addition, the COGCC does not allow injection into the Precambrian crystalline basement formations, unless it can be proven that the potential for induced seismicity is low [*COGCC*, 2016].

Reactive responses, in contrast, happen once the induced seismicity has begun. Reactive responses can include change in the injection well operation parameters such as reduced injection rate or a change in the injection depth interval. In addition, a reactive response may include the complete shutdown of one or more injection well operations. "Traffic-light" systems are sometimes used to trigger reactive measures [*Ellsworth*, 2013; *Bommer et al*., 2015; *McGarr et al*., 2015]. In a traffic-light system, regulatory agency required action, i.e., lowering injection rates or stopping injection, that is taken when earthquakes of a certain number or magnitude occur [*Ellsworth*, 2013; *McGarr et al*., 2015]. The effectiveness of these systems is often limited by sparse seismic network coverage that results in a relatively high-magnitude detection threshold [*Ellsworth*, 2013].

Greeley, Colorado (Figure 1), has been the focus of injection-induced seismicity research since the occurrence of an M_w 3.2 earthquake in June 2014 [*Yeck et al*., 2016] and is a good case for studying the effectiveness of induced seismicity mitigation. Following the earthquakes, reactive mitigation measures included concreting the bottom of the well and temporary reduction of injection rates. Disposal well NGL-C4A was the closest well to the earthquake and had a high injection rate (between 250,000 and 364,000 barrels per month (bbl/month) during the previous 10 months); therefore, NGL-C4A was identified as the likely cause of the induced seismicity. Tests following the June 2014 earthquake of NGL-C4A found the lowest section of the injection interval to be highly fractured. In order to reduce a possible hydraulic connection between the injection formations and the crystalline basement, the bottom of NGL-C4A was cemented [*Yeck et al*., 2016]. When additional felt events occurred in August 2016, similar mitigation efforts were taken at two addition disposal wells near the seismicity, EWS-2, and HPD Kersey 1 (Figure 1). Here we use numerical groundwater models to determine if the mitigation efforts were effective. We model the pore pressure change caused by injection from 22 wastewater injection wells within 30 km of the seismicity to determine the relative contribution of injection of Greeley Wells close to the seismicity ($<$15 km) and the Far-field Wells farther from the seismicity (15–30 km). The change in the injection interval caused by the cementing the bottom of the well, the main mitigation action, is also captured during the modeling.

2. Study Site Background

Greeley, Colorado (Figure 1), is located near the north-south trending axis of the asymmetrical Denver-Julesburg (DJ) Basin (also called Denver Basin). The DJ Basin, a Laramide-age structure, is approximately 180,000 km^2 in eastern Colorado, extending into Wyoming and Nebraska [*Higley and Cox*, 2007]. Oil and gas produced in the DJ Basin, the majority of which is in Colorado, is a major contributor to Colorado's total oil and gas production annually. The DJ Basin has produced hydrocarbons since 1881, when the first well was drilled in the basin [*Higley and Cox*, 2007]. During the production of hydrocarbons, a large amount of wastewater is generated and must be disposed of either through wastewater disposal wells, wastewater recycling, or trucking of wastewater elsewhere. Wastewater disposal via Underground Injection Control Program Class II wastewater disposal wells is the leading disposal method near Greeley, Colorado. Currently, there are over 30 disposal wells near Greeley (Figure 1) injecting into the Denver Basin combined disposal zone. The Denver Basin combined disposal zone is a sedimentary interval of approximately 500 m thick, composed of the Permian Lyons sandstone Formation, the interbedded sandstone and carbonate Wolfcamp and Ingleside Formations, and the Pennsylvanian Fountain coarse-grained arkose Formation (Table 1). The Denver Basin combined disposal zone is directly underlain by the Precambrian crystalline basement. A small number of the disposal wells (six) inject into only the upper Denver Basin combined disposal

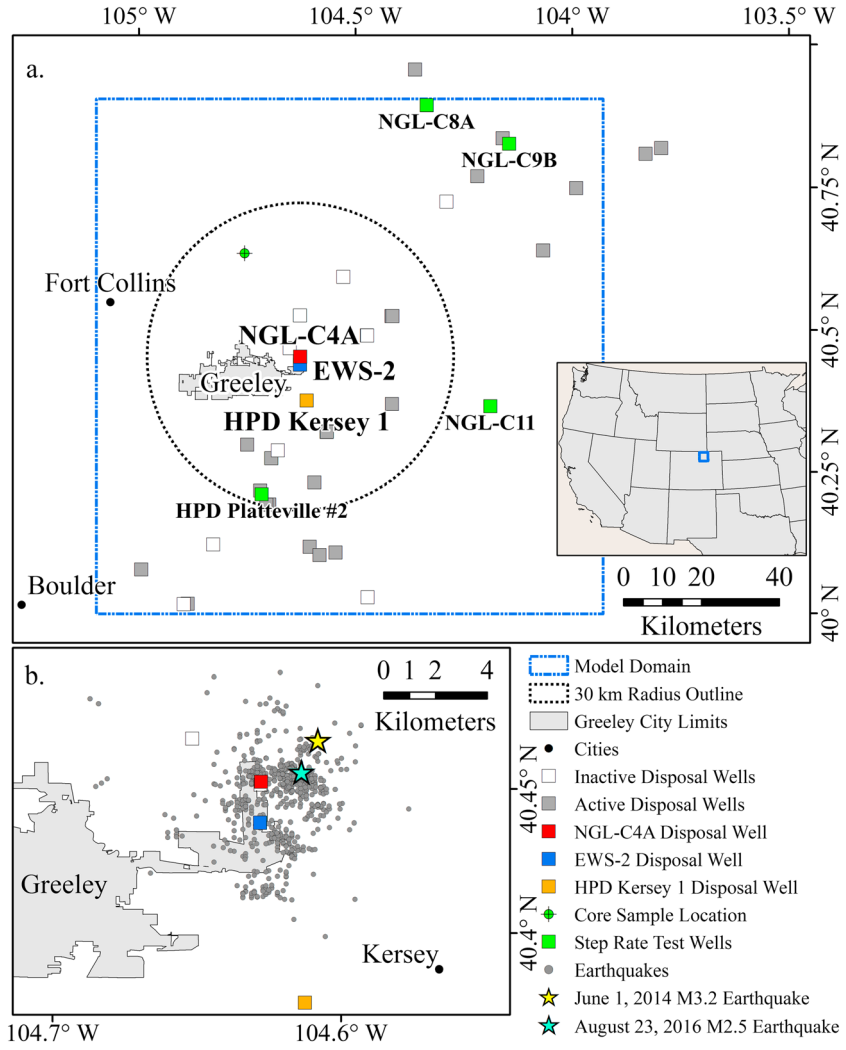

Figure 1. Study area. (a) Wastewater disposal wells (squares) within Weld County, Colorado. Disposal Wells that were involved in mitigation efforts are NGL-C4A in red, EWS-2 in blue, and HPD Kersey 1 in orange. Step Rate Test reanalysis wells are marked in green. The well location for the core used in constant-head permeameter tests is marked in green circle with cross. The model domain is outlined in dashed-blue, and the 30 km radius circle centered on the center of seismicity is in dashed-black. (b) Seismicity from June 2014 to August 2016. The yellow star indicates the location of the 1 June 2014 M_w 3.2 earthquake, and the blue star indicates the location of the felt earthquakes on 23 August 2016. Earthquake data between November 2013 and April 2015 are from *Yeck et al.* [2016].

Table 1. Denver Basin Combined Disposal Zone Lithology

Formation	Dominate Lithology	Approximate Thickness (m)
Confining Layer		
Lykins	Mudstone	190
Injection Interval		
Lyons	Sandstone	95
Lower Satanka	Shale	91
Wolfcamp	Sandstone and carbonate	107
Ingleside	Sandstone and carbonate	80
Fountain	Coarse-grained arkose	170
Basement		
Precambrian Basement	Crystalline basement	not available

zone (Lyons Formation), while the majority of the disposal wells inject into the entire disposal zone (Lyons through Fountain Formations).

An M_w 3.2 earthquake occurred near Greeley on 1 June 2014 (Figure 1b). Prior to this earthquake, the area had not experienced a reported earthquake for more than 41 years [*Yeck et al*., 2016]. Following the earthquake, University of Colorado Boulder researchers deployed six seismometers to monitor the seismicity in the area. Injection volumes, well logs, and injection tests were obtained from publicly available sources at the Colorado Oil and Gas Conservation Commission [*COGCC*, 2016]. The earthquake occurred close to the wastewater disposal well NGL-C4A, which started injection in April 2013 and injected consistently over 250,000 bbl/month, with a maximum rate of 363,888 bbl/month, from August 2013 to June 2014. *Weingarten et al*. [2015] studied the relationships between wastewater disposal well injection parameters and seismicity in the central United States and showed a statistically significant correlation between high injection rate (>300,000 bbl/month) and occurrence of earthquakes.

NGL-C4A was the closest well to the M_w 3.2 earthquake and had the highest injection rate among the wells near Greeley. This disposal well became the focus of the investigation and seismicity mitigation efforts. *Yeck et al*. [2016] used subspace detection methods to determine when the earthquakes began and found seismicity commenced in November 2013, several months following the initial injection at NGL-C4A. Prior to November 2013, no earthquakes occurred within the Greeley area, which is further confirmed by no seismicity detected from 2008–2010 in the small-magnitude seismicity catalog from *Nakai et al*. [2017]. In addition, drilling logs and a spinner survey (a downhole measurement of fluid velocity with depth) conducted on NGL-C4A after the June 2014 earthquake suggest a highly fractured interval in the mid-to-lower Fountain Formation that was receiving the majority of the injected wastewater. Additional events in June 2014 prompted the COGCC to require the NGL-C4A Well to be shut-in. To mitigate hydraulic connection between the injection interval and the basement, the bottom 500 feet (152.4 m) of the well was plugged with cement [*Yeck et al*., 2016]. After the plugging, injection resumed into the interval above the cemented section. The resumed injection followed a tiered injection rate scheme: slowly increasing injection rate over time. In addition, seismic monitoring by the operators around new disposal wells with injection rates >10,000 bbl/d (~300,000 bbl/month) was instituted as a precautionary measure.

Induced earthquakes can occur at distances of greater than 20 or 30 km from the wastewater disposal wells [*Keranen et al*., 2014; *Block et al*., 2015]. Within 30 km of the induced seismicity, a total of 22 wastewater disposal wells (Table 2 and Figure 1) are injecting or have injected into the Denver Basin combine disposal zone. The majority of the disposal wells inject into the entire Denver Basin combined disposal zone, but six inject into only the upper Denver Basin combined disposal zone, the Lyons Formation. The first injection within the 30 km radius began in January 1999; nine of the wells began injection after the June 2014 earthquake. To determine how much impact the injection from the additional wells has on pore pressure change, we modeled the pore pressure generated from injection of the 22 wells from January 1999 through August 2016 using a 3-D numerical groundwater model of the basin.

3. Wastewater Injection and Seismicity Data

Taking into account all the wells within 30 km of the seismicity, the total injection rate has been over 1 million bbl/month since 2009 and consistently over two million bbl/month since 2012 (Figure 2a). Between the start of injection at NGL-C4A and the June 2014 earthquake, the averaged total injection rate for all wells was approximately three million bbl/month. Between June 2014 and August 2016, when another felt sequence of earthquakes occurred, the average injection rate for all wells has been over four million bbl/month.

Seismicity in the area visually correlates with the injection rate of the seven Greeley Wells that are within 15 km of the seismicity with only short time lags of approximately a few months between the peak injection months and increased seismicity (Figure 2b). The data are for the entire period over which both the injection data and seismicity data are available. Seismicity began in November 2013 [*Yeck et al*., 2016] and continues through the present. Seismicity decreased after the felt sequence in June 2014 corresponding with the decreased injection rates. Seismicity increased again in January 2015, shortly after the injection of the Greeley Wells exceeded 500,000 bbl/month. Another peak in seismicity occurred in April 2015, shortly after injection reached 490,000 bbl/month. Spatially, there is not a clear diffusion front in the seismicity migration.

Table 2. Denver Basin Combined Disposal Zone Wastewater Disposal Wells Within 30 km of Seismicity[a]

Well Name	API	Date of Injection	Distance From NGL-C4A [km]	Latitude	Longitude	Disposal Zone
NGL-C4A	0512335841	Apr 2013 to Present	0.00	40.45	−104.63	Denver Basin combined disposal zone
NGL C4	0512312448	Oct 2004 to Nov 2014	0.11	40.45	−104.63	Upper Denver Basin combined disposal zone
EWS 2 [former Triton #2]	0512337808	May 2015 to Present	1.58	40.44	−104.63	Denver Basin combined disposal zone
Johnson 22-34I	0512326604	Mar 2008 to Feb 2010	2.62	40.47	−104.65	Upper Denver Basin combined disposal zone
NGL-C10	0512340772	Feb 2016 to Present	8.08	40.53	−104.63	Denver Basin combined disposal zone
HPD Kersey 1	0512327116	Jan 2010 to Present	8.62	40.38	−104.61	Denver Basin combined disposal zone
Synergy Disposal 15–18 I	0512325694	Nov 2008 to May 2015	13.69	40.49	−104.47	Upper Denver Basin combined disposal zone
Conquest SWD 1–8	0512316804	Jan 1999 to Nov 2007	15.52	40.32	−104.57	Upper Denver Basin combined disposal zone
NGL-C1B	0512329536	Mar 2009 to Present	15.53	40.32	−104.57	Denver Basin combined disposal zone
NGL-C1C	0512340377	Mar 2015 to Present	15.57	40.32	−104.57	Denver Basin combined disposal zone
NGL C1A (SWD 1-8A)	0512323038	Jan 2006 to Present	15.59	40.32	−104.57	Upper Denver Basin combined disposal zone
NGL-C7A	0512332207	Mar 2011 to Present	19.54	40.52	−104.42	Denver Basin combined disposal zone
NGL-C7B	0512334520	Aug 2014 to Present	19.72	40.52	−104.41	Denver Basin combined disposal zone
EWS-3 [former Triton 1]	0512337120	Sep 2014 to Present	20.05	40.30	−104.75	Denver Basin combined disposal zone
NGL-C12	0512341201	Oct 2015 to Present	20.16	40.37	−104.42	Denver Basin combined disposal zone
NGL-C3A	0512331735	Oct 2014 to Present	20.64	40.27	−104.69	Denver Basin combined disposal zone
NGL C3 [Geraldine 32–1]	0512319688	Jan 2000 to Feb 2015	20.65	40.27	−104.69	Upper Denver Basin combined disposal zone
LSWD-1	0512330367	Apr 2012 to Present	24.77	40.23	−104.59	Denver Basin combined disposal zone
HPD Platteville #1	0512329168	Jan 2010 to Present	27.34	40.22	−104.72	Denver Basin combined disposal zone
HPD Platteville #2	0512339710	Mar 2015 to Present	28.00	40.21	−104.72	Denver Basin combined disposal zone
NGL-C6	0512326004	Nov 2007 to Present	29.58	40.19	−104.70	Denver Basin combined disposal zone
NGL-C6A	0512340968	May 2015 to Present	29.74	40.19	−104.71	Denver Basin combined disposal zone

[a]Data from *COGCC* [2016] listed in order of distance from NGL-C4A. Greeley Wells, within 15 km of seismicity, are shaded grey.

The seismic data are from *Yeck et al*. [2016] and this study with varying magnitudes of completeness. We determined the magnitude of completeness, the minimum magnitude of complete earthquake record in a catalog, using the maximum curvature method [*Wiemer and Wyss*, 2000; *Woessner and Wiemer*, 2005]. A conservative magnitude of completeness for all the data sets is *M* 1.0. Figure 2 presents the pattern of correlation between the injection rates and the seismicity above the magnitude of completeness *M* 1.0.

Currently, four of the original six seismometers installed near NGL-C4A continue to monitor seismicity in the area. Two of the original six seismometers were removed in April 2015, and one of the remaining four seismometers was relocated in June 2016. Between May 2016 and August 2016, an additional nine seismometers were installed in the area. We also installed one seismometer at the Rocky Mountain Arsenal National Wildlife Refuge, approximately 65 km southwest of Greeley.

4. Hydrologic Parameters

Hydrologic parameters are needed for modeling of pore pressure generated from injection. To estimate hydrologic parameters for the injection interval, we reanalyzed step rate test data on four wells with injection intervals in the Denver Basin combined disposal zone (Figure 1a) and conducted constant-head permeameter tests on core samples from the injection interval units. The step rate test data are obtained from the *COGCC* [2016]. We took core samples from the 1UPPR-Ferch Core (Figure 1a) stored at the U.S. Geological Survey's Core Research Center [*USGS CRC*, 2016].

4.1. Step Rate Test as Variable Rate Injection Test

Step rate tests are conducted on injection wells during the well permitting process to determine the injection interval's fracture parting pressure—the pressure at which preexisting fractures extend or new fractures form within the formation. During a step rate test, pressure in the injection well is initially allowed to equilibrate to formation pressure [*Singh et al*., 1987]. A variable rate injection test is then performed in a step rate fashion using steps of equal time length and increasing injection rate. The length of the time step is chosen such that the bottom-hole pressure is stabilized at the end of each time step, for wells near Greeley usually less than 30 min. Data recorded are the injection rate and well bottom-hole pressure. The injection rate versus the stabilized bottom-hole pressure data are expected to be linear with a constant slope until the fracture parting

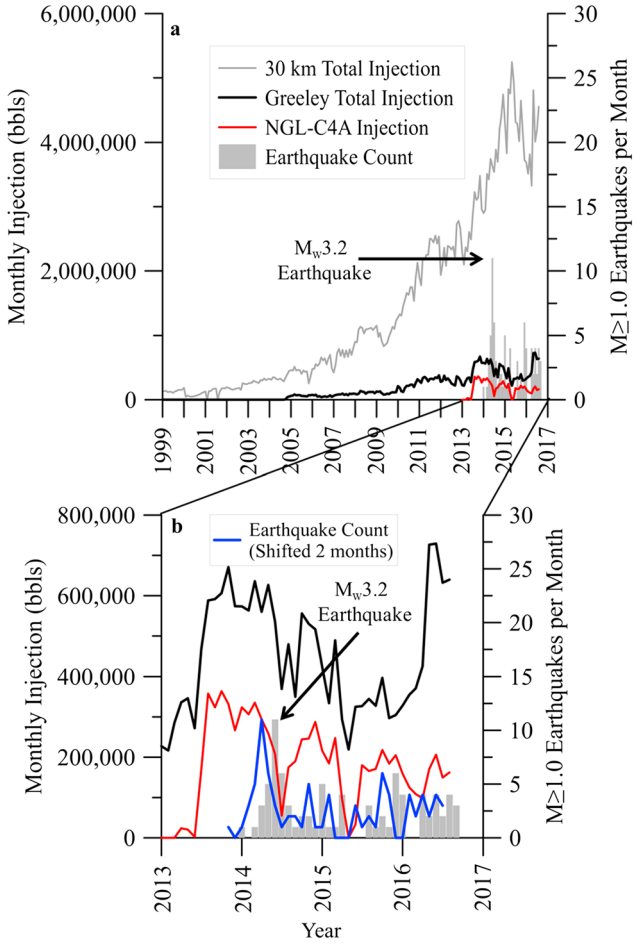

Figure 2. Injection and seismicity $M > 1.0$ history. (a) History of wastewater injection, into the Denver Basin combined disposal zone, within 30 km of the area of seismicity. The grey line represents the total monthly injection for all the wells; the black line is the total monthly injection for the Greeley Wells. The bar graph represents the earthquakes per month. (b) Total monthly injection for the Greeley Wells and earthquakes per month for January 2013 through August 2016. The blue line represents the earthquakes per month shifted 2 months to show the approximate lag in the correlation between the injection and seismicity. Earthquake data between November 2013 and April 2015 are from *Yeck et al.* [2016].

pressure is reached. Once the fracture parting pressure is reached, fractures are created and they act as higher permeability conduits for fluid and pressures are lowered, resulting in a reduced slope.

We analyzed the step rate test data from four wells, HPD Platteville #2, NGL-C11, NGL-C8A, and NGL-C9B (Figure 1a), as a step-drawdown test, which is a variable rate pumping test used to determine hydrologic properties under different pumping conditions. The data are from the *COGCC* [2016] well files for the four disposal wells. Step rate and step-drawdown tests have similar procedures although one test injects (step rate test) while the other pumps (step-drawdown test). Since the two tests have a procedure of step rate injection/pumping, the same equation that solves the step-drawdown test can be used on data from the step rate test to estimate hydraulic conductivity. The sign on the pumping rate and the change in hydraulic head are just reversed for injection and increasing hydraulic head.

We use the program AQTESOLV [*Duffield*, 2006] for the analysis. AQTESOLV solves for transmissivity and storativity using a modified version of the Theis method [*Theis*, 1935] for step-drawdown tests in confined aquifers; we use this method for single-well tests assuming fully penetrating wells and taking into account linear and nonlinear well losses [*Bear*, 1979 p. 374–375]:

$$\Delta h = \frac{Q}{4\pi T}[w(u) + 2S_w] + CQ^P \tag{1}$$

$$w(u) = \int_u^\infty \frac{e^{-x}}{x} dx \tag{2}$$

$$u = \frac{r^2 S}{4Tt} \tag{3}$$

where Δh is change in hydraulic head in the pumped/injected well (L), Q is pumping or injection rate ($L^3\,T^{-1}$), T is transmissivity ($L^2\,T^{-1}$), S_w is the wellbore skin factor (1), CQ^P is nonlinear well loss (L), $w(u)$ is the well function (1), u is a dimensionless time parameter (1), x is the variable of integration (1), r is radial distance of influence (L), S is storativity (1), and t is time (T). The radius of the well is used for the radial distance when analyzing single-well tests in AQETSOLV. Single-well tests estimate transmissivity well, but storativity values are hard to estimate from due to the well losses [*Jacob*, 1947; *Agarwal et al.*, 1970; *Renard et al.*, 2009]. The wellbore skin factor S_w relates to the change in permeability of the formation at the borehole due to

damage during drilling or well completion [*Bear*, 1979]. Positive wellbore skin factors indicate that the damaged area has a lower hydraulic conductivity than the actual formation; negative wellbore skin factors indicate that the damaged area has a higher hydraulic conductivity than the actual formation [*Yang and Gates*, 1997]. The well loss constant C takes into account the well's construction (e.g., screen, liner, and gravel pack) and the quality of its completion.

By varying the nonlinear well loss variables, we found that the transmissivity is insensitive to the nonlinear well loss. We used several skin factors during analysis to achieve the best solution. We included an anisotropy ratio, vertical hydraulic conductivity over horizontal hydraulic conductivity (K_v/K_h), of 1:10 in the analysis, which was confirmed by the constant-head permeameter testing (see section 4.2). Using the thickness of the injection interval, we calculated the hydraulic conductivity for the disposal zone in each well.

The hydraulic conductivity ranges from approximately 10^{-8} to 10^{-7} m s^{-1}. We note that while solution (1) assumes a homogeneous aquifer, the step rate tests were conducted over the entire injection interval, which includes numerous formations of varying composition, including sandstones and carbonates. The entire injection interval therefore can be heterogeneous. The hydraulic conductivity results between the wells that are located across the basin are consistent.

4.2. Constant-Head Permeameter Tests

We conducted constant-head permeameter tests on samples collected from core drilled in the DJ Basin and stored at the USGS CRC in Denver, Colorado. The core samples are from the 1 UPPR-Ferch Well (Figure 1a) that was cored through all of the geologic units of the Denver Basin combined disposal zone. We took samples from the Lyons, Wolfcamp, Ingleside, and Fountain Formations. These formations are largely sandstones, but there are some carbonates interbedded within the Wolfcamp and Ingleside Formations. The samples were picked based on previous permeability values estimated by petrophysical service companies [*USGS CRC*, 2016]. We chose samples of relatively higher permeability estimates as those intervals are where most of the injection fluid will go within the heterogeneous injection interval.

The USGS CRC cut the core samples to a diameter of 2.5 cm. We secured the 10 samples in PVC pipe for testing on a Trautwein M100000 Standard Panel permeameter. We saturated the samples by allowing at least 50 mL of water, which is greater than 25 pore volumes, to flow through the sample. We then ran multiple constant-head tests by measuring the time for at least 20 mL of water to flow through the sample. We calculated the hydraulic conductivity of each test using a variation of Darcy's law [*Freeze and Cherry*, 1979]:

$$K = \frac{VL}{\pi r^2 ht} \tag{4}$$

where K is hydraulic conductivity in the direction of flow (L T^{-1}), V is volume of fluid discharged (L^3), L is sample length (L), r is sample radius (L), h is the constant head difference maintained across the sample (L), and t is time (T). The results range from 10^{-10} to 10^{-6} m s^{-1}. These values are consistent with the hydraulic conductivities used by *Belitz and Bredehoeft* [1988] to model groundwater flow in the DJ Basin aquifers. We conducted tests on three sets of samples, one from the Lyons Formation, one from the Ingleside Formation, and one from the Fountain Formation, to measure the vertical and horizontal hydraulic conductivities from the same interval. The anisotropy (K_v/K_h) was 0.16 for the Lyons sandstone samples, 0.06 for the Ingleside sandstone/carbonate samples, and 0.19 for the Fountain coarse-grained arkose samples. The disparity in anisotropy values is likely due to the differences in lithology of the three formations or natural variation between the samples. However, the difference in the anisotropy values is only within one order of magnitude.

5. Groundwater Modeling of Pore Pressure Distribution Generated by Injection

5.1. Model Setup

We modeled the change in pore pressure caused by wastewater injection from the 22 wells within a 30 km radius of the Greeley seismicity using the USGS 3-D finite difference model MODFLOW-2005. MODFLOW solves the 3-D transient groundwater flow equation for hydraulic head [*McDonald and Harbaugh*, 1988]:

$$S_s \frac{\partial h}{\partial t} = \frac{\partial}{\partial x}\left(K_x \frac{\partial h}{\partial x}\right) + \frac{\partial}{\partial y}\left(K_y \frac{\partial h}{\partial y}\right) + \frac{\partial}{\partial z}\left(K_z \frac{\partial h}{\partial z}\right) + Q \tag{5}$$

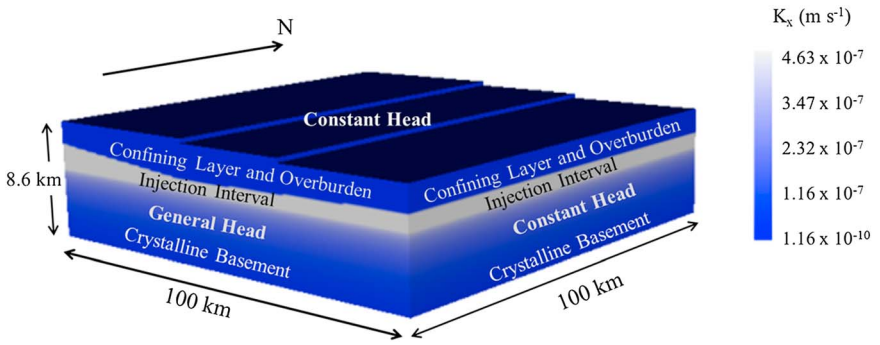

Figure 3. Model setup. The west and east boundaries have a constant head boundary condition. The model top follows local topography and is a constant head boundary. The south boundary is a general head boundary, and the north boundary (not shown) is a no-flow boundary. In all of the model runs, horizontal hydraulic conductivities K_x and K_y are equal, and the basement horizontal hydraulic conductivity decreases exponentially with depth. K_z is equal to K_x in the modeled scenarios shown in Figure 4. However, vertical anisotropy, K_z/K_x, is varied during the sensitivity analyses.

where S_s is specific storage (L^{-1}); h is hydraulic head (L); t is time (T); K_x, K_y, and K_z are hydraulic conductivity in the x, y, and z directions ($L\ T^{-1}$); and Q is the volumetric flux per unit volume of sources and/or sinks (T^{-1}). Change in hydraulic head is calculated by subtracting the head at each time step by the initial conditions (steady state conditions). We converted the change in hydraulic head into pore pressure change using the specific weight conversion:

$$\Delta P = \gamma \Delta h \tag{6}$$

where ΔP is pore pressure change ($MLT^{-2}\ L^{-2}$), γ is the specific weight of water ($MLT^{-2}\ L^{-3}$), and Δh is hydraulic head change (L).

We created a 3-D model of 100 km by 100 km by 8.6 km that captures the asymmetric nature of the Denver Basin combined disposal zone formations (Figure 3). The model domain is large to reduce the effect of boundary conditions on the changes caused by the injection of the wells near the center of the model domain. We assigned constant head boundaries to the east and west sides of the domain with constant heads consistent with the hydraulic head measurements given for the units in *Belitz and Bredehoeft* [1988]. This constant head condition ensures a background regional flow of the injection interval from west to east. We set a general-head boundary on the south boundary. General-head boundaries are head-dependent flux boundaries where the flux is dependent on the difference between the simulated head inside the boundary and a specified head at a certain distance beyond the boundary. The specified head are those on the southernmost part of the DJ Basin obtained from the modeling study of *Belitz and Bredehoeft* [1988]. A no-flow boundary is assigned to the north boundary since the boundary is far enough from the injection that the modeled pore pressure change caused by injection is not affected by the boundary conditions. We assigned a constant head boundary on the model top to simulate a constant water table that follows the topography at the surface of the model domain.

As a base case, we set an isotropic, homogeneous hydraulic conductivity of the Denver Basin combined disposal zone (injection interval) to 4.6×10^{-7} m s^{-1}. This value is on the high end of the permeameter test results, which ranged from 10^{-10} to 10^{-7} m s^{-1}, and is consistent with the step rate test as variable rate injection test analysis, which ranged from 10^{-8} to 10^{-7} m s^{-1}. *Schulze-Makuch et al*. [1999] showed that in heterogeneous systems hydraulic conductivity scales with the volume of the tested sample. Therefore, larger volume pumping (or injection) tests are a more representative estimation of the aquifer parameters than small volume permeameter tests. While there is likely lateral heterogeneity throughout the Denver Basin, the results from the step rate test analyses are consistent and cover a wide area across the basin. In addition, the hydraulic conductivities calculated from the constant-head permeameter testing are also consistent with the step rate test estimations. The consistency in the estimated values from different wells across such a wide area supports our choice to model the injection interval as a homogeneous unit.

We assigned a hydraulic conductivity of 1.6×10^{-10} m s^{-1} to the confining layer, the Lykins mudstone Formation, above the injection interval. We assigned a hydraulic conductivity the same as the injection

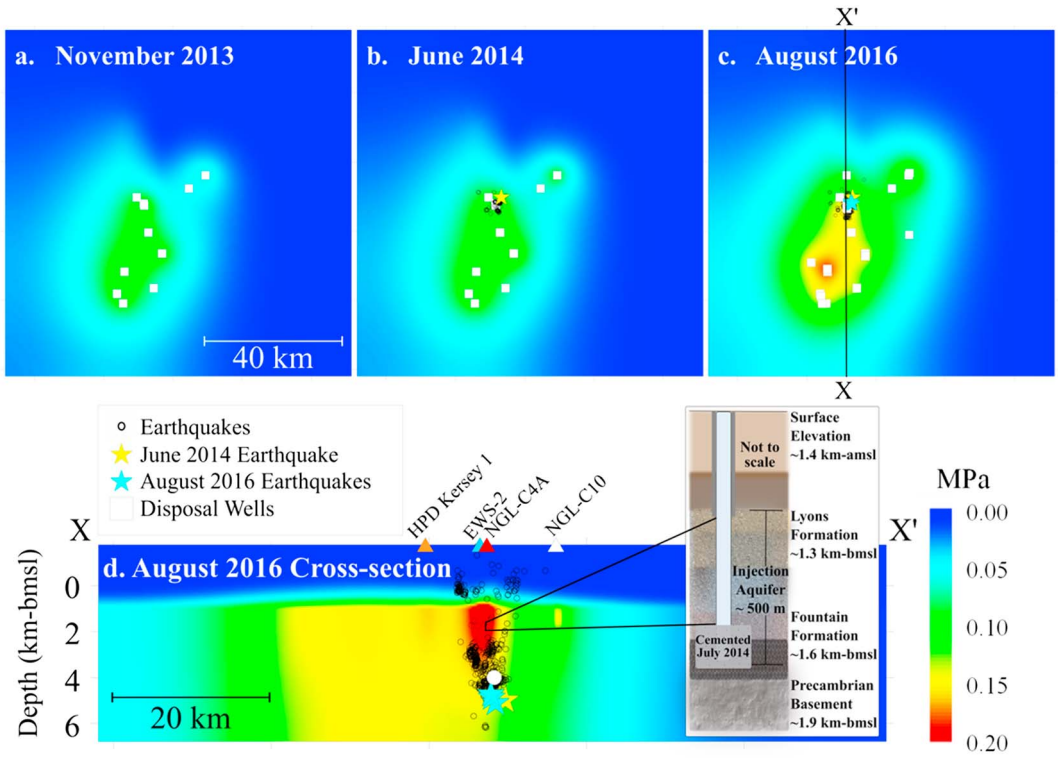

Figure 4. Modeled pore pressure results viewed at 4 km bmsl. Wastewater disposal wells are labeled in white squares. (a) Pore pressure for November 2013. (b) June 2014 pore pressure with June 2014 earthquakes in black circles and the 1 June 2014 M_w 3.2 earthquake indicated by the yellow star. (c) Pore pressure for August 2016 with all earthquakes since June 2014 in black circles and August 2016 felt earthquakes as blue stars. (d.) Cross section X-X′ with earthquakes projected onto the cross section. The line X-X′ is the location of the cross section in Figure 4d. The main grouping of seismicity starts directly below the bottom of the injection interval (~1.7–1.9 km bsl) and extends deeper into the basement. The white dot, approximately 2–2.5 km below the injection interval, is the location of model estimates shown in Figures 5 and 6. Earthquake locations from June 2014 through April 2015 are from *Yeck et al.* [2016]. Surface locations of wastewater injection wells close to the cross section are labeled with triangles. An inset of a generalized well diagram of NGL-C4A with main injection interval formations labeled is included to illustrate the Denver Basin combined disposal zone. The well diagram is modified from *Yeck et al.* [2016].

interval to the top of the crystalline basement and decreased the conductivity of the basement exponentially with depth [*Manning and Ingebritsen*, 1999]. We assigned a specific storage of 10^{-7} m^{-1}, which is in the range of values estimated in the step rate test as a variable rate injection test analysis and is consistent with values in the literature for the injection intervals [*Colorado Division of Water Resources*, 1976]. We ran the model under steady state conditions without injection to acquire initial head conditions for the transient model. The initial hydraulic heads approximate the potentiometric surface from *Belitz and Bredehoeft* [1988] of the injection interval units that is a result of steady state regional groundwater flow modeling study.

We placed the wells in our model based on the well logs provided by the *COGCC* [2016]. We assign the injection interval of NGL-C4A to reflect the change in the injection interval following the cementation of the bottom in June 2014. We used the injection records from the COGCC to calculate the injection rate through time for each of the 22 wells. The injection volume and number of injection days are reported to the COGCC on a monthly basis, and we estimated the daily injection rate by dividing the injection volume by number of injection days. We ran the model from 1 January 1999 through 31 August 2016. Each of the 22 wells inject for at least a portion of the time.

5.2. Pore Pressure Model Results

We present the modeled pore pressure change (Figure 4a) for November 2013, when the seismicity began; June 2014 (Figure 4b), when the M_w 3.2 earthquake occurred; and August 2016 (Figure 4c), when an addition felt sequence of earthquakes occurred. Most of the seismicity occurred between 2 and 5 km below mean sea

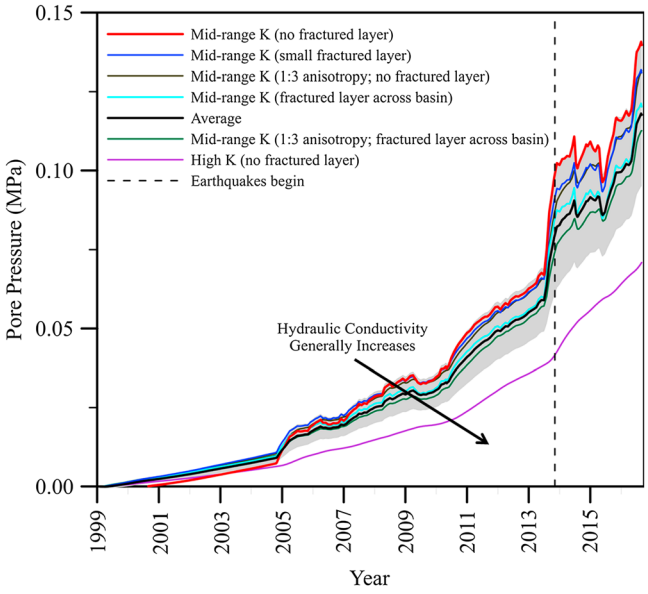

Figure 5. Pore pressure change (MPa) through time at a location in the area of seismicity, located at white dot in Figure 4d. The colored lines each represent one scenario in the sensitivity analysis. The dark black line represents the average of the pore pressure change, and the grey area is ±1 standard deviation. The thicker red line is the model results shown in Figures 4 and 6. The vertical dashed line is November 2013, when seismicity began.

level (bmsl) (3.4–6.4 km belowground surface) with the majority of the earthquakes occurring at approximately 4.25 km bmsl [*Yeck et al.*, 2016] (5.6 km belowground surface). Therefore, we present the pore pressure change at 4 km bmsl (~5.4 km belowground surface) (Figures 4a–4c).

The earthquakes prior to June 2014 were detected using subspace detection methods applied to two regional seismic stations, >100 km from the events [*Yeck et al.*, 2016]. We assume that the detected November 2013 earthquakes are in the same area of the first locatable earthquakes (June 2014) based on the waveforms matching during the subspace detection. Therefore, the November 2013 earthquakes all occur in the area where model results predicted an increase in pore pressure of approximately 0.10 MPa (Figure 4a). The June 2014 earthquakes (Figure 4b) also occur within the area of approximately 0.10 MPa of pore pressure increase. By August 2016, the area where seismicity occurs has a pore pressure increase of approximately 0.15 MPa (Figure 4c). The north-south cross section in Figure 4d, through the area of seismicity and NGL-C4A, shows that the injection interval experiences a much larger increase in pore pressure than the crystalline basement where the majority of the earthquakes occur. In addition, the increased pore pressure extends deep into the basement and to the south of the injection wells. The injection wells closest to the cross section are indicated in Figure 4d by triangles at the surface of the model.

These results are from the base case scenario with midrange hydraulic conductivity in the injection interval, no anisotropy, and no fractured (higher hydraulic conductivity) layer. We tested other scenarios during the sensitivity analysis. We performed sensitivity analyses of the model for a range of hydraulic conductivities obtained from the permeameter tests and step rate tests analysis. In addition, we ran the model with combinations of anisotropy and the presence of a high hydraulic conductivity fractured layer near NGL-C4A and across the entire basin (Figure 5), a feature inferred from the well logs and the spinner survey conducted on NGL-C4A. Model results using the lowest hydraulic conductivity values for the injection interval produced unrealistically high pore pressure changes and therefore are not presented. Figure 5 presents the pore pressure change at a location (shown in Figure 4d) near the majority of the earthquakes for each of the sensitivity analysis results. Excluding the highest hydraulic conductivity scenario, the pore pressure near the majority of the earthquakes increases in the sensitivity analysis to at least 0.08 MPa by November 2013 when the seismicity started.

We also ran the model, using the base case parameters as used to attain the results shown in Figure 4, with only the Greeley Wells injecting, only NGL-C4A, and only the Far-field Wells between 15 and 30 km from the seismicity injecting to determine the relative contribution of these wells to the total pore pressure increase at a single location (shown in Figure 4d) near the majority of the earthquakes. The results are presented in Figure 6. Figure 6a shows a pore pressure increase of approximately 0.10 MPa in November 2013 when all wells within 30 km of radius inject. Figure 6b shows that 68% of the pore pressure increase in November 2013 is attributed to the Greeley Wells (which includes NGL-C4A) and 34% of the pore pressure increase in November 2013 is attributed to NGL-C4A alone. Figure 6c shows the pore pressure increase caused by injection at the Far-field Wells both from the modeled far-field injection and from subtracting the model results of

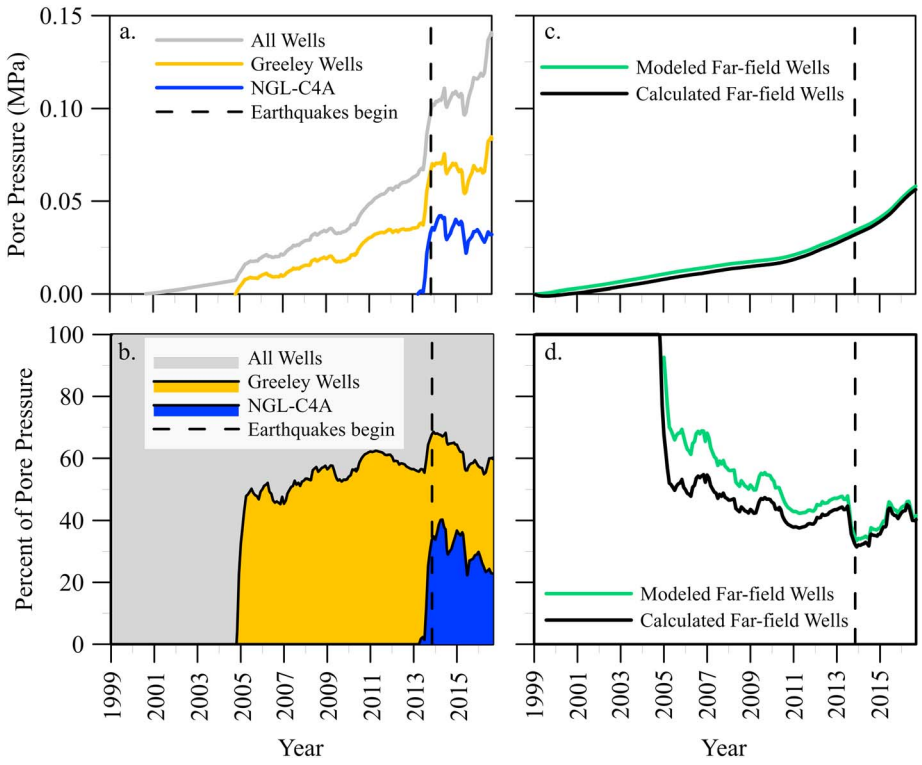

Figure 6. Well contributions to pore pressure change at a location in the area of seismicity, located at white dot in Figure 4d. (a) Pore pressure change (MPa) through time for all wells (grey), only Greeley Wells (orange), and only NGL-C4A (blue). (b) The percent of the total pore pressure change by well grouping. The grey color represents 100% of the pore pressure change from all the wells. The orange color represents the percent of the total pore pressure change from only the Greeley Wells (within 15 km). The blue color represents the percent of the total pore pressure change from only NGL-C4A. (c) Pore pressure change (MPa) through time for the far-field wells (15–30 km from the seismicity). The green line represents the pore pressure change results when only the injection of the far-field wells is modeled. The black line represents the pore pressure change caused by the injection of the far-field wells calculated from the difference between the modeled results for injection of all the wells and modeled results for injection of only the Greeley Wells. (d) The percent of the total pore pressure change for the far-field wells. The vertical black dashed line is November 2013, when seismicity began.

the only Greeley Wells injecting from the results of all wells injecting (Calculated Far-field). The percentage of the modeled total pore pressure increase due to injection of the Far-field Wells is also presented in Figure 6d. The results in Figures 6c and 6d show a small difference between the modeled and calculated far-field results. We also assess the influence of the well groupings by averaging the percentages of pore pressure increase for each well grouping's modeled results. The Far-field Well grouping's averaged percentage was calculated using the percentage difference between the all well injection model results and the only Greeley Wells injection model results. On average, the Greeley Wells (including NGL-C4A) contribute 56% of the pore pressure, NGL-C4A contributes 28% of the pore pressure, and the Far-field Wells contribute 44% of the pore pressure.

6. Discussion

The pore pressure modeling results show that the pore pressure increase to approximately 0.10 MPa coincided with the commencement of seismicity in November 2013. This pore pressure increase is similar to the suggested triggering threshold in Oklahoma of approximately 0.07 MPa [*Keranen et al.*, 2014]. It is also within the range of pore pressure increase, 0.01 to 0.20 MPa, modeled for Azle, Texas, by *Hornbach et al.* [2015]. In addition to studies of induced seismicity, studies of dynamic triggering [e.g., *Hill*, 2008] and Coulomb stress transfer [e.g., *King et al.*, 1994; *Stein*, 1999] indicate that very small changes in stress can promote or prohibit seismicity. If faults in the crust are critically stressed [*Townend and Zoback*, 2000], then a site-specific critical pore pressure change threshold is a reasonable assumption. *Hsieh and Bredehoeft* [1981] also

asserted that a critical threshold was consistent with the theory of *Hubbert and Rubey* [1959] on fluid pressure's role on fault mechanics, the theoretical framework used by *Healy et al.* [1968] to explain the mechanism of the Denver earthquakes.

Analysis of the likely in situ stress field was not conducted as part of this study due to scarce existing data preventing a thorough mapping of the local stress field. However, the fault movement and orientation are consistent with the regional stress field. *Dart* [1985] found the mean minimum horizontal stress orientation of the Denver-Julesburg Basin to be between N73E and N76E, based on borehole breakouts. The moment tensor solution for the June 2014 M_w 3.2 earthquake shows a normal faulting event with north-northwest striking nodal planes [*Herrmann*, 2016]. Northwest striking normal faults are consistent with the current stress field.

In 1999–2004, prior to the Greeley Wells injecting, pore pressure increases near the seismicity were predicted by the model as less than 0.01 MPa (Figure 6a). NGL-C4, almost co-located with NGL-C4A and one of the Greeley Wells (Table 2), started injection in October 2004. The injection rate rapidly increased across the area in mid-2009, which leads to an increase in pore pressure near the location of the future seismicity. However, pore pressure did not significantly increase near the area of future seismicity until NGL-C4A began injection in April 2013. The first seismicity in November 2013 and the June 2014 M_w 3.2 earthquake followed the dramatic increase in pore pressure to approximately 0.10 MPa. Pore pressures continue to generally increase from the start of seismicity in November 2013 through the second felt earthquake sequence in August 2016, reaching the model predicted estimate of approximately 0.14 MPa near the location of the seismicity (Figures 5 and 6a).

From June 2014 to April 2016, the combined injection rates of the Greeley Wells fluctuate, ranging between approximately 220,000 bbl/month and 556,000 bbl/month. Following April 2016, there is a general increase in injection rate until June 2016, when the rate reached a new maximum combined rate of 729,375 bbl/month (Figure 2b). The Greeley Wells, including NGL-C4A, account for on average 56% of the pore pressure increase (Figure 6b). NGL-C4A alone accounts for on average 28% of the pore pressure increase. Therefore, the six wells near Greeley (not including NGL-C4A) are responsible for on average 28% of the pore pressure increase. The relative contributions to the pore pressure by each grouping of wells are a function of the injection rate and distance from the seismicity. From the modeled results, the Far-field Wells have less influence on the area near seismicity when the Greeley Wells are injecting than when they are not (Figures 6c and 6d). However, the overall influence of the Far-field Wells does not change much whether the Greeley Wells closer to the seismicity are injecting or not.

An interesting observation is that the largest pore pressure increase is not in the area of the seismicity, but farther south near the well with the highest average injection rate during 2016. The reason for the lack of seismicity in the large area of increased pore pressure could be due to multiple factors. We can speculate that faults on which the seismicity would occur are not present, or not optimally oriented for failure, or not critically stressed.

6.1. Reactive Mitigation

Mitigation efforts in Greeley, Colorado, following felt earthquakes have focused on individual wells. Following the June 2014 M_w 3.2 earthquake, the operator of NGL-C4A cemented the bottom 500 feet (152.4 m) of the well. Injection resumed in July 2014 at an allowable rate of 5000 bbl/d (~150,000 bbl/month). The rate was increased in steps reaching a rate close to the injection rates prior to the earthquake. The allowable injection rate increased in August 2014 to 7500 bbl/d (~225,000 bbl/month), in October 2014 to 9500 bbl/d (~285,000 bbl/month), and in December 2014 to 12,000 bbl/d (~360,000 bbl/month). The actual injection rate at NGL-C4A, between July 2014 and December 2014, did not exceed 288,000 bbl/month.

Since June 2014, the average injection rate at NGL-C4A has decreased, but the injection rate at a nearby Greeley Well, HPD Kersey 1, has stayed consistent. In addition, another operator installed a new well, EWS-2, less than 2 km from NGL-C4A that started injection in May 2015 and injects at relatively high rates (maximum of ~312,000 bbl/month). In August 2016, a series of felt earthquakes occurred near Greeley [*Did You Feel It? (DYFI)*, 2016]. The largest earthquake in the series was a local magnitude (M_L) 2.5 followed by a M_L 2.3 several hours later. After these earthquakes, the COGCC required the operators of the two closest wells to NGL-C4A, EWS-2, and HPD Kersey 1, to plug the bottom of the wells with cement. The bottom 372 feet

(~113 m) of EWS-2 was cemented in late August 2016, and the bottom 498 feet (~151.8 m) of HPD Kersey 1 was cemented in October 2016 [*COGCC*, 2016]. Injection resumed at EWS-2 and HPD Kersey 1 directly following the plugging of the bottom of the wells. EWS-2 resumed injection at a rate of ~160,000 bbl/month, and HPD Kersey 1 resumed injection at a rate of ~82,000 bbl/month [*COGCC*, 2016]. On 6 November 2016, another series of felt earthquakes occurred [*DYFI*, 2016]; the largest of which were two earthquakes 5 s apart, a M_L 2.7 followed by a M_L 3.0.

Based on the occurrence of seismicity that continues, cementing the bottom of the wells has not stopped or reduced seismicity. *Weingarten et al*. [2015] suggested a statistically significant link between injection rate and induced seismicity. Other sites of induced seismicity, e.g., Rocky Mountain Arsenal, Colorado [*Healy et al*., 1968; *Hsieh and Bredehoeft*, 1981]; Rangely, Colorado [*Raleigh et al*., 1976]; and Oklahoma sites [*Langenbruch and Zoback*, 2016], have seen reduced seismicity rates with reduction of injection rates. Since over half of the pore pressure increase can be attributed to the Greeley Wells (Figure 6b and Table 2), reducing the rates at these wells will likely be a more effective approach in minimizing the pore pressure increase and therefore reducing the chance of triggering the seismicity. Reducing the rates of wells or larger well spacing overall, therefore effectively reducing the aggregate injection rate, may not be feasible for a variety of reasons. Recommending a specific well spacing or spatially limited injection rate, i.e., an injection rate per square kilometer injection, would be largely site specific and be heavily influenced by the local hydraulic parameters [*Weingarten and Ge*, 2015]. In addition, a thorough cost-benefit analysis would be needed to determine if the well spacing and injection rate limitations were possible.

7. Conclusions

Pore pressure modeling shows that the Greeley area seismicity began after the pore pressure increase reached approximately 0.10 MPa in the area of activity. The largest contribution to pore pressure increase, on average 56% in the area of seismicity, is from the seven Greeley Wells that are within 15 km of the seismic area. However, the wells between 15 and 30 km of the center of seismicity still contributed a substantial portion, on average 44%, of the pore pressure increase near the seismicity. Our results show not only the influence of injection on pore pressure at short distances from the earthquakes but also the significant contribution to pore pressure change by injection at all distances modeled, up to 30 km, from the earthquakes.

Our modeling shows that pore pressure increase from injection could reach 0.15 MPa without a permeable pathway such as a fault or fractured zone. This magnitude of pore pressure increase has been shown in other studies to be sufficient to induce seismicity [*Ogwari and Horton*, 2016; *Hornbach et al*., 2015; *Keranen et al*., 2014]. In addition, sensitivity analysis of hydraulic conductivity shows that pore pressure in the area of seismicity could increase to a level that induces earthquakes for the range of hydraulic conductivity in the area.

The local seismic network continues to detect seismicity in the area despite mitigation efforts, such as the cementing of the bottom of the injection interval. Our model results indicate the pore pressure continues to increase with continued injection near the seismicity. Mitigation by cementing wells in Greeley has been ineffective in reducing the number or magnitude of earthquakes. Since over 50% of the pore pressure increase in the area of seismicity can be attributed to the Greeley Wells, a more effective approach may include reduction of injection rates at these wells. Furthermore, the Far-field Wells between 15 and 30 km from the seismicity contribute approximately 44% of the pore pressure increase. This is a significant portion of the total increase in pore pressure. An appropriate preventative mitigation action may include larger spacing between wells. Farther well spacing would reduce the number of wells within a prescribed distance such that the spatial aggregation of the injection rate would be much smaller. Mitigating induced seismicity may require hard decisions about economic and physical feasibility. A cost-benefit analysis of the number of wells, well spacing, and injection rate limitation would be necessary to examine the feasibility of various scenarios.

Acknowledgments

Funding for this work was provided by USGS National Earthquake Hazards Reduction Program (NEHRP) grant G13AC00023 and by National Science Foundation (NSF) Award EAR 1520846 (Hazards SEES). We thank the USGS Core Research Center for samples of the 1 UPPR-Ferch Well (CRC Library Number E053) and David Budd for his help choosing core samples. We thank Mazi-Mathias Onyeali for his help with the constant-head permeameter tests. We thank Incorporated Research Institutions for Seismology–Portable Array Seismic Studies of the Continental Lithosphere (IRIS-PASSCAL) for the seismic instruments used in this study. Jefferson Yarce played an important role by helping with earthquake locations during summer 2016. In addition, Justin Ball and Kyren Bogolub managed the seismometer deployment, and Daniel Feucht, Daniel Zietlow, Jefferson Yarce, Steven Plescia, and Enrique Chon assisted with seismometer deployment. William Yeck and Harley Benz with the USGS and Stuart Ellsworth and Chris Eisinger with the COGCC assisted with planning the seismometer deployment. David Ketchum with the USGS assisted with telemetry for the seismic network. We thank the landowners who allowed us to place the seismometers on their property. In addition, we thank U.S. Fish and Wildlife, Rocky Mountain Arsenal (RMA) Wildlife Refuge, and former Deputy Project Leader Bruce Hastings for allowing and assisting with the placement of a seismic station at the RMA Wildlife Refuge. We also thank Matthew Weingarten who provided valuable suggestions for the groundwater modeling and data collection. We thank the two anonymous reviewers for providing constructive comments and suggestions that greatly improved the paper. Wastewater injection data and step rate test data are available by searching the API numbers of each well through the COGCC website http://cogcc.state.co.us/data.html#/cogis, the constant-head permeameter results are available on the USGS CRC website (CRC Library Number E053) https://my.usgs.gov/crcwc/, and seismic data are archived with IRIS.

References

Agarwal, R. G., R. Al-Hussainy, and H. J. J. Ramey (1970), An investigation of wellbore storage and skin effect in unsteady liquid flow: I. Analytical treatment, *Soc. Pet. Eng. J.*, *10*, 279–290.

Bear, J. (1979), *Hydraulics of Groundwater*, McGraw-Hill, New York.

Belitz, K., and J. D. Bredehoeft (1988), Hydrodynamics of Denver Basin: Explanation of subnormal fluid pressures, *Am. Assoc. Pet. Geol. Bull.*, *72*(11), 1334–1359, doi:10.1306/703C999C-1707-11D7-8645000102C1865D.

Block, L. V., C. K. Wood, W. L. Yeck, and V. M. King (2015), Induced seismicity constraints on subsurface geological structure, Paradox Valley, Colorado, *Geophys. J. Int.*, *200*(2), 1170–1193, doi:10.1093/gji/ggu459.
Bommer, J. J., H. Crowley, and R. Pinho (2015), A risk-mitigation approach to the management of induced seismicity, *J. Seismol.*, *19*(2), 623–646, doi:10.1007/s10950-015-9478-z.
COGCC (2016), Colorado Oil & Gas Conservation Commission. [Available at http://cogcc.state.co.us/data.html#/cogis.]
Colorado Division of Water Resources (1976), *Ground Water Resources of the Bedrock Aquifers of the Denver Basin, Colorado*, Dep. Nat. Resour., Denver, Colo.
Dart, R. (1985), Horizontal-stress directions in the Denver and Illinois Basins from the orientation of borehole breakouts, *U.S. Geol. Surv. Rep.* pp. 85–733, Denver, Colo.
Duffield, G. M. (2006), *AQTESOLV for Windows Version 4 User's Guide*, HydroSOLVE, Inc., Reston, Va.
DYFI (2016), USGS Did You Feel It? reports. [Available at https://earthquake.usgs.gov/data/dyfi/.]
Ellsworth, W. L. (2013), Injection-induced earthquakes, *Science*, *341*(6142), 1225942, doi:10.1126/science.1225942.
Freeze, R. A., and J. A. Cherry (1979), *Groundwater*, Prentice-Hall, Englewood Cliffs, N. J.
Healy, J. H., W. W. Rubey, D. T. Griggs, and C. B. Raleigh (1968), The Denver earthquakes, *Science*, *161*(3848), 1301–1310.
Herrmann, R. (2016), North America moment tensor 1995–2016, accessed May 11, 2017, from St. Louis University web site. [Available at http://www.eas.slu.edu/eqc/eqc_mt/MECH.NA/20140601033521/index.html, Updated December 7, 2015.]
Higley, D. K., and D. O. Cox (2007), *Oil and Gas Exploration and Development Along the Front Range in the Denver Basin of Colorado, Nebraska, and Wyoming*, *U.S. Geol. Surv. Digital Data Ser.*, pp. 1–40, Reston, Va., doi:10.1017/CBO9781107415324.004.
Hill, D. P. (2008), Dynamic stresses, coulomb failure, and remote triggering, *Bull. Seismol. Soc. Am.*, *98*, 66–92, doi:10.1785/0120070049.
Hornbach, M. J., et al. (2015), Causal factors for seismicity near Azle, Texas, *Nat. Commun.*, *6*, 6728, doi:10.1038/ncomms7728.
Hsieh, P. A., and J. D. Bredehoeft (1981), A reservoir analysis of the Denver earthquakes: A case of induced seismicity, *J. Geophys. Res.*, *86*, 903–920, doi:10.1029/JB086iB02p00903.
Hubbert, M. K., and W. W. Rubey (1959), Role of fluid pressure in mechanics of overthrust faulting, *Geol. Soc. Am. Bull.*, *70*, 115–206.
Jacob, C. E. (1947), Drawdown test to determine effective radius of artesian well, *Trans. Am. Soc. Civ. Eng.*, *112*, 1047–1064.
Keranen, K. M., M. Weingarten, G. A. Abers, B. A. Bekins, and S. Ge (2014), Induced earthquakes. Sharp increase in central Oklahoma seismicity since 2008 induced by massive wastewater injection, *Science*, *345*(6195), 448–451, doi:10.1126/science.1255802.
Kim, W.-Y. (2013), Induced seismicity associated with fluid injection into a deep well in Youngstown, Ohio, *J. Geophys. Res. Solid Earth*, *118*, 3506–3518, doi:10.1002/jgrb.50247.
King, G. C. P., R. S. Stein, and J. Lin (1994), Static stress changes and the triggering of earthquakes, *Bull. Seismol. Soc. Am.*, *84*, 935–953.
Langenbruch, C., and M. D. Zoback (2016), How will induced seismicity in Oklahoma respond to decreased saltwater injection rates? *Sci. Adv.*, *2*(e1601542), 1–9, doi:10.1126/sciadv.1601542.
Manning, C. E., and S. E. Ingebritsen (1999), Permeability of the continental crust: Implications of geothermal data and metamorphic systems, *Rev. Geophys.*, *37*, 127–150, doi:10.1029/1998RG900002.
McDonald, M. G., and A. W. Harbaugh (1988), A modular three-dimensional finite-difference ground-water flow model investigations, U.S. Geol. Surv. Tech. Water Resour. Invest., 06-A1, 586 p.
McGarr, A., et al. (2015), Coping with earthquakes induced by fluid injection, *Science*, *347*(6224), 830–831, doi:10.1126/science.aaa0494.
Nakai, J. S., A. F. Sheehan, and S. L. Bilek (2017), Seismicity of the rocky mountains and Rio Grande Rift from the EarthScope Transportable Array and CREST temporary seismic networks, 2008–2010, *J. Geophys. Res. Solid Earth*, *122*, 2173–2192, doi:10.1002/2016JB013389.
Ogwari, P. O., and S. P. Horton (2016), Numerical model of pore-pressure diffusion associated with the initiation of the 2010-2011 Guy-Greenbrier, Arkansas earthquakes, *Geofluids*, *16*, 954–970, doi:10.1111/gfl.12198.
Raleigh, C. B., J. H. Healy, and J. D. Bredehoeft (1976), An experiment in earthquake control at Rangely, Colorado, *Science*, *191*(4233), 1230–1237, doi:10.1126/science.191.4233.1230.
Renard, P., D. Glenz, and M. Mejias (2009), Understanding diagnostic plots for well-test interpretation, *Hydrogeol. J.*, *17*(3), 589–600.
Schulze-Makuch, D., D. A. Carlson, D. S. Cherkauer, and P. Malik (1999), Scale dependency of hydraulic conductivity in heterogeneous media, *Groundwater*, *37*(6), 904–919, doi:10.1111/j.1745-6584.1999.tb01190.x.
Singh, P. K., R. G. Agarwal, and L. D. Krase (1987), Systematic design and analysis of step-rate test to determine formation parting pressure, SPE, 16798, pp. 491–503, Society of Petroleum Engineers.
Stein, R. S. (1999), The role of stress transfer in earthquake occurrence, *Nature*, *402*, 605–609.
Theis, C. V. (1935), The relation between the lowering of the Piezometric surface and the rate and duration of discharge of a well using ground-water storage, *Eos Trans. AGU*, *16*(2), 519, doi:10.1029/TR016i002p00519.
Townend, J., and M. D. Zoback (2000), How faulting keeps the crust strong, *Geology*, *28*(5), 399–402.
USGS CRC (2016), USGS Core Research Center. [Available at https://geology.cr.usgs.gov/crc/.]
Weingarten, M., and S. Ge (2015), Hydrogeologic modeling aimed at optimizing injection well operation in a hypothetical multi-injection well reservoir: Implications for induced seismicity, Abstract S13B-2820 presented at 2015 Fall Meeting, AGU, San Francisco, Calif., 14–18 Dec.
Weingarten, M., S. Ge, J. W. Godt, B. A. Bekins, and J. L. Rubinstein (2015), High-rate injection is associated with the increase in U.S. mid-continent seismicity, *Science*, *348*(6241), 1336–1340, doi:10.1126/science.aab1345.
Wiemer, S., and M. Wyss (2000), Minimum magnitude of completeness in earthquake catalogs: Examples from Alaska, the western United States, and Japan, *Bull. Seismol. Soc. Am.*, *90*(4), 859–869, doi:10.1785/0119990114.
Woessner, J., and S. Wiemer (2005), Assessing the quality of earthquake catalogues: Estimating the magnitude of completeness and its uncertainty, *Bull. Seismol. Soc. Am.*, *95*(2), 684–698, doi:10.1785/0120040007.
Yang, Y. J., and T. M. Gates (1997), Wellbore skin effect in slug-test data analysis for low permeability geologic materials, *Groundwater*, *35*(6), 931–937.
Yeck, W. L., A. F. Sheehan, H. M. Benz, M. Weingarten, and J. Nakai (2016), Rapid response, monitoring, and mitigation of induced seismicity near Greeley, Colorado, *Seismol. Res. Lett.*, *87*(4), 837–847, doi:10.1785/0220150275.
Yeck, W. L., G. P. Hayes, D. E. McNamara, J. L. Rubinstein, W. D. Barnhart, P. S. Earle, and H. M. Benz (2017), Oklahoma experiences largest earthquake during ongoing regional wastewater injection hazard mitigation efforts, *Geophys. Res. Lett.*, *44*, 711–717, doi:10.1002/2016GL071685.